Kinetics of Substitution of Weakly Coordinating Nitrate by Chloride in (η^5-Cp)Ru(CO)(ER_3)ONO_2 (ER_3 = $AsPh_3$, PPh_3, P(*p*-anisyl)$_3$, PPh_2(*o*-anisyl), P(OPh)$_3$) in Dichloromethane

Minhton Cao, Liem V. Do, Norris W. Hoffman,* Man-Lung Kwan, Julie K. Little, J. Michael McGilvray, Christopher B. Morris, Bjorn C. Söderberg, and Andrzej Wierzbicki

Department of Chemistry, University of South Alabama, Mobile, Alabama 36688

Thomas R. Cundari

CROMIUM and the Department of Chemistry, University of Memphis, Memphis, Tennessee 38152

Charles H. Lake

Departments of Chemistry, University of Alabama at Birmingham, Birmingham, Alabama 35294, and Indiana University of Pennsylvania, Indiana, Pennsylvania 15705

Edward. J. Valente

Department of Chemistry, Mississippi College, Box 4065, Clinton, Mississippi 39058

Received August 4, 2000

The d^6 complexes of formula (η^5-Cp)Ru(CO)(ER_3)ONO_2, where ER_3 = $AsPh_3$, PPh_3, P(*p*-anisyl)$_3$, PPh_2(*o*-anisyl), and P(OPh)$_3$, were prepared by reaction of their chloro analogues with $AgNO_3$ in CH_2Cl_2. They underwent moderately slow substitution of the relatively weakly coordinating nitrate by chloride in dry CH_2Cl_2 in the presence of excess $[N(PPh_3)_2^+]Cl^-$. A kinetics study showed the reaction to be first order in nitrato complex and independent of chloride salt concentration under pseudo-first-order conditions. First-order rate constants for nitrate metathesis follow the trend P(OPh)$_3$ < PPh_3 < P(*p*-anisyl)$_3$ < $AsPh_3$ ≪ PPh_2(*o*-anisyl), with k_1 at 25 °C for the first four in the series from 1.4 to 4.4 × 10^{-5} s^{-1}. Activation parameters for conversion of (η^5-Cp)Ru(CO)($AsPh_3$)ONO_2 to its chloride are $\Delta H^{\ddagger}$ = 17(2) kcal/mol and $\Delta S^{\ddagger}$ = −21(5) eu. Even use of a slightly moist solvent increased the rate of nitrate metathesis by 20−30% without changing the form of the rate law. The complex containing PPh_2(*o*-anisyl) was approximately 2 orders of magnitude more reactive (k_1 = 4.9 × 10^{-3} s^{-1}). A likely explanation is stabilization of a coordinatively unsaturated intermediate by weak coordination of the potentially chelating *o*-OMe group. A mechanism entailing rate-limiting conversion of the neutral nitrato complex into a coordinatively unsaturated ion-paired species is consistent with this set of data. Semiempirical calculations (PM3(tm)), which model the structures of complexes in these systems quite well, supported such behavior. X-ray crystal structures were determined for the $AsPh_3$ nitrato and chloro complexes and for the PPh_3 chloro complex.

Introduction

Transition-metal complexes of weakly coordinating anions have received extensive scrutiny for their ability to promote carbon−carbon bond formation with special reactivity and selectivity in the reactions of olefins.[1] Such complexes often provide excellent Lewis acid sites for catalysis of olefin polymerization and oligomerization. Given the general desirability of controlling the electron-richness of low-valent metal systems, tuning electron density at a metal center (in addition to use of phosphorus, carbenoid, and similar neutral ligands) via uninegative ligands ranging in donor power from isocyanate[2] down to recently designed extremely weakly coordinating anions[3] such as teflate, $CB_{11}H_{12}^-$, and fluorinated derivatives of BPh_4^- has considerable merit. Relatively little research has been conducted on reactivity patterns of complexes containing moderately weakly

(1) Tempel, D. J.; Johnson, L. K.; Huff, R. L.; White, P. S.; Brookhart, M. *J. Am. Chem. Soc.* **2000**, *122*, 6686.

(2) Araghizadeh, F.; Branan, D. M.; Hoffman, N. W.; Jones, J. H.; McElroy, E. A.; Miller, N. C.; Ramage, D. L.; Salazar, A. B.; Young, S. H. *Inorg. Chem.* **1988**, *27*, 3752.

(3) (a) Lupinetti, A. J.; Strauss, S. H. *Chemtracts-Inorg. Chem.* **1972**, *11*, 565. (b) Strauss, S. H. *Chem. Rev.* **1993**, *93*, 927.

10.1021/om000670d CCC: $20.00
Publication on Web 05/03/2001

coordinating anions such as ONO_2^- and $O_2PF_2^-$.[4] Ruthenium(II) is a d^6 system generally slow to undergo ligand substitution reactions unless weakly coordinating ligands are present. We report here a study of the kinetics of nitrate-anion replacement in the pseudo-octahedral system (η^5-Cp)Ru(CO)(ER_3)ONO_2 by chloride from $[N(PPh_3)_2^+]Cl^-$ (abbreviated hereafter as $(PPN^+)Cl^-$) in the weakly polar solvent CH_2Cl_2.

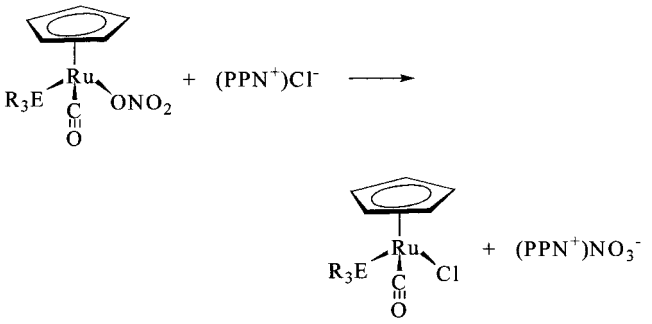

Experimental Section

Starting Materials. Tertiary phosphines, $P(OPh)_3$, and $AsPh_3$ were purchased from Strem Chemicals and used as received. (η^5-Cp)Ru$(CO)_2$Cl was prepared according to the procedure of Humphries and Knox from $Ru_3(CO)_{12}$ (Strem).[5] Reagent toluene, heptane, and diethyl ether (Mallinckrodt) were used as received. Reagent dichloromethane (Mallinckrodt) for synthetic purposes was stored over 4 Å molecular sieves in air. That for kinetics was dried 4 days and then stored under N_2 over 4 Å molecular sieves which had been dried by heating 2 days at 130 °C/20 mTorr). $(PPN^+)Cl^-$ (Strem) was recrystallized from dichloromethane/diethyl ether, heated at 90 °C/20 mTorr, and stored under N_2.

General Spectrometric Procedures. FTIR spectra were recorded in 2.5-mm and 5-mm path length CaF_2 cells in dichloromethane solution. NMR spectra of $CDCl_3$ solutions were recorded at 90 MHz. ^1H and ^{13}C chemical shifts are relative to respective internal TMS, and ^{31}P chemical shifts are relative to external 85% aqueous H_3PO_4. ^{13}C signals for the carbonyl ligands were not recorded due to the time required to afford useful signal-to-noise ratios. The more important IR and NMR spectroscopic parameters for compounds **1**−**10** are presented in Table 1; others are listed with their respective compounds below in this section. UV−visible spectra were run in dichloromethane solution in quartz 1-cm cuvettes on a Shimadzu 2100 spectrometer fitted with multiple-cell changer and thermoelectric temperature control.

(η^5-Cp)Ru(CO)($AsPh_3$)Cl (1). Synthesis of this chloride and its phosphorus-ligand analogues was similar to that described in the literature,[6] except that toluene instead of xylenes was used as solvent. A solution initially containing $CpRu(CO)_2Cl$ (129 mg, 0.500 mmol) and $AsPh_3$ (168 mg, 0.549 mmol) in 50 mL of toluene was heated under nitrogen at reflux for 30 h. The resulting clear yellow solution was cooled and then handled aerobically. It was concentrated to about 5 mL under reduced pressure. To the resulting yellow-orange liquid was added dropwise 3 mL of diethyl ether and then 40 mL of heptane. The microcrystalline yellow-orange precipitate afforded was filtered, washed with four 5-mL portions of heptane, and then dried overnight in vacuo. Yield 233 mg (86.9%). Anal. Calcd for $C_{24}H_{20}AsClORu$: C 53.80; H 3.76. Found: C 53.61; H 3.78. $AsPh_3$-ligand NMR: ^1H δ 7.48 (m); ^{13}C δ 134.4, 132.9, 130.1, 128.8. Single crystals for X-ray analysis were grown by vapor diffusion of pentane into a toluene solution (ca. 5 mg in 12 mL).

The chloro compounds **2**−**5** were prepared in analogous fashion on a similar scale, with yields in the 79−91% range.

(η^5-Cp)Ru(CO)(PPh_3)Cl (2). Yellow-orange microcrystals. Its spectroscopic data matched those previously reported.[5] Single crystals for X-ray analysis were grown by vapor diffusion of pentane into a toluene solution (ca. 5 mg in 12 mL).

(η^5-Cp)Ru(CO)(P(*p*-anisyl)$_3$)Cl (3). Lemon-yellow microcrystals. Anal. Calcd for $C_{27}H_{26}ClO_4PRu$: C 55.72; H 4.50. Found: C 55.58; H 4.49. P(*p*-anisyl)$_3$-ligand NMR: ^1H δ 7.48 (d, 8.8 Hz, 6H), 6.89 (d, 8.8 Hz, 6H), 3.82 (s, 9H); ^{13}C δ 161.0, 135.0, 126.7, 113.8.

(η^5-Cp)Ru(CO)(PPh_2(*o*-anisyl))Cl (4). Lemon-yellow microcrystals. Anal. Calcd for $C_{25}H_{22}ClO_2PRu$: C 57.53; H 4.25; Found C 57.38; H 4.24. PPh_2(*o*-anisyl)$_3$-ligand NMR: ^1H δ 7.8−7.3 (m, 9H), 6.90 (m, 3H), 3.60 (s, 3H); ^{13}C δ 160.3, 135.3, 134.7, 134.0, 133.6, 132.8, 132.2, 130.2, 129.8, 128.4, 128.2, 127.9, 127.7, 120.5, 110.9, 54.8.

(η^5-Cp)Ru(CO)(P(OPh)$_3$)Cl (5). Pale-yellow microcrystals. Its spectroscopic data matched those previously reported.[6b]

(η^5-Cp)Ru(CO)($AsPh_3$)ONO_2 (6). Complex **1** (102 mg, 0.198 mmol) was stirred with $AgNO_3$ (43.7 mg, 0.248 mmol) in 20 mL of CH_2Cl_2 for 18 h protected from light. Although the reaction mixture was prepared aerobically, the flask in which it was stirred was blanketed by nitrogen to avoid exposure to excess moisture. Then the mixture was filtered through Celite and concentrated to about 3 mL under reduced pressure. Into the resulting yellow-orange solution were dripped 3 mL of diethyl ether and then 40 mL of heptane. The microcrystalline yellow-orange precipitate afforded was filtered, washed with four 5-mL portions of heptane, and then dried overnight in vacuo. Yield 88 mg (82%). Anal. Calcd for $C_{24}H_{20}AsNO_4Ru$: C 51.26; H 3.58. Found: C 51.13; H 3.56. $AsPh_3$-ligand NMR: ^1H δ 7.41 (m); ^{13}C δ 134.3, 132.8, 130.5, 129.1. Single crystals for X-ray analysis were grown by vapor diffusion of hexanes into a toluene solution (ca. 5 mg in 10 mL).

The nitrato complexes **7**−**10** were prepared in analogous fashion on a similar scale, with yields in the 77−89% range.

(η^5-Cp)Ru(CO)(PPh_3)ONO_2 (7). Yellow-orange microcrystals. Anal. Calcd for $C_{24}H_{20}NO_4PRu$: C 55.60; H 3.89. Found: C 55.77; H 3.92. PPh_3-ligand NMR: ^1H δ 7.44 (m); ^{13}C δ 133.4, 130.8, 128.7.

(η^5-Cp)Ru(CO)(P(*p*-anisyl)$_3$)ONO_2 (8). Yellow-orange microcrystals. Anal. Calcd for $C_{27}H_{26}NO_7PRu$: C 55.72; H 4.50. Found: C 55.58; H 4.49. P(*p*-anisyl)$_3$-ligand NMR: ^1H δ 7.41 (m, 9H), 6.92 (m, 6H), 3.62 (s, 9H); ^{13}C δ 161.3, 134.8, 125.1, 114.1, 55.2.

(η^5-Cp)Ru(CO)(PPh_2(*o*-anisyl))ONO_2 (9). Yellow-orange microcrystals. Anal. Calcd for $C_{25}H_{22}NO_5PRu$: C 57.74; H 4.04. Found: C 57.45; H 4.07. PPh_2(*o*-anisyl)$_3$-ligand NMR: ^1H δ 7.41 (m, 9H), 6.92 (m, 3H), 3.29 (s, 3H); ^{13}C δ 160.6, 134.2, 133.8, 133.0, 132.6, 130.7, 130.6, 130.2, 128.7, 128.4, 128.1, 55.0.

(η^5-Cp)Ru(CO)(P(OPh)$_3$)ONO_2 (10). Pale-yellow microcrystals. Anal. Calcd for $C_{24}H_{20}NO_7PRu$: C 50.89; H 3.56. Found: C 50.61; H 3.52. P(OPh)$_3$-ligand NMR: ^1H δ 7.32 (m); ^{13}C δ 151.0, 129.8, 125.6, 121.4.

(η^5-Cp)Ru(CO)(PPh_2(*o*-anisyl))Br (11). Nitrate **9** (109.7 mg, 0.2000 mmol) was dissolved in 10 mL methanol. To the resulting yellow-orange solution was added solid NaBr (52.7 mg, 0.512 mmol). Stirring of the mixture for 15 min produced a microcrystalline yellow solid in a yellow liquid. Slow dropwise addition of 30 mL of deionized water afforded more solid and an essentially colorless liquid. The lemon-yellow solid was

(4) Branan, D. M.; Hoffman, N. W.; McElroy, A. E.; Prokopuk, N. C.; Robbins, M. J.; Hill, W. E.; Webb, T. R. *Inorg. Chem.* **1991**, *30*, 1200 and references therein.

(5) Humphries, A. P.; Knox, S. A. R. *J. Chem. Soc., Dalton Trans.* **1975**, 1710.

(6) Earlier studies have used xylene at reflux. (a) Brown, D. A.; Lyons, H. J.; Manning, A. R. *Inorg. Chim. Acta* **1970**, *4*, 428. (b) Brown, D. A.; Lyons, H. J.; Sane, R. T. *Inorg. Chim. Acta* **1970**, *4*, 621. (c) Jungbauer, A.; Behrens, H. *Z. Naturforsch., Teil B* **1978**, *33*, 1083.

filtered, washed with 3:1 (v/v) water/methanol, and then dried first in air and next at 50 °C/50 mTorr. Yield 94.2 mg (83.2%). Anal. Calcd for $C_{25}H_{22}BrO_2PRu$: C 53.02; H 3.92. Found: C 53.08; H 4.04. PPh_2(*o*-anisyl)$_3$-ligand NMR: ^{1}H δ 7.8−7.3 (m, 9H), 6.90 (m, 3H), 3.60 (s, 3H); ^{13}C δ 160.0, 135.1, 133.8, 132.8, 132.5, 132.8, 130.3, 129.9, 128.3, 127.9, 127.0, 117.2, 111.0, 54.9.

UV−Visible Kinetics Experiments. Although the reaction mixtures were not sensitive to O_2, they were prepared and handled under N_2 to rigorously minimize exposure to water. All glassware and the quartz cuvettes were heated for at least 6 h in an oven at 150 °C. Upon their removal hot from the oven, they were exposed to an N_2 atmosphere so that any surface making contact with the reaction mixtures could transfer essentially no water. Dichloromethane dried as previously described over molecular sieves afforded results identical to those when it was dried by prolonged reflux over and distillation from CaH_2. The cuvettes were placed into large-neck Schlenk tubes under N_2, reaction mixtures were transferred in by cannulae, and the cuvettes were tightly sealed with Teflon stoppers and then inserted into the spectrometer's thermostated cell-holder. For each nitrato complex, the reaction was first monitored by repetitive scans at appropriate intervals over 550−350 nm to ensure clean isosbestic behavior and to determine the optimum wavelength at which to monitor absorbance over time. All experiments were run under pseudo-first-order conditions, with $[(PPN^+)X^-]_o/[CpRu(CO)(ER_3)\text{-}ONO_2]_o$ ratio ≥ 10 (X = Cl for all five nitrates; X = Br for only nitrate **9**). Fixed-wavelength absorbance versus time runs employed three mixtures of different initial-concentration ratios run simultaneously using the cell-changer. An example for complex **6** below provides sufficient detail to describe our techniques.

UV−Visible Monitoring of Kinetics of Conversion of Nitrate 6 into Chloride 1. Into an oven-dried Schlenk tube under N_2 containing a Teflon-coated magnetic stirbar was placed 52.2 mg (0.0910 mmol) $(PPN^+)Cl^-$ weighed under N_2 (if weighed in air, its mass slowly increased as it picked up water from lab air of ca. 70% relative humidity). Next 5.1 mg (0.0091 mmol) **6** (weighed in air) was poured into the tube and 10.0 mL of dry dichloromethane was added by volumetric pipet (taken hot from oven, with all liquid-contact surfaces shielded from air). As soon as the reactants had dissolved, a portion of the reaction mixture was transferred under N_2 by cannula into a dry cuvette. The cuvette was then stoppered and placed into the thermostated cell-holder set for 25.0 °C; after allowing 4 min for the solution to reach constant temperature, scans over 550−350 nm were run automatically every 10.8 min for 18 h. Spectral overlay (see Figure 1) of selected scans showed clean isosbestic behavior. For determination of pseudo-first-order rate constants and dependence upon $[(PPN^+)Cl^-]$, 50.0 mL of an 0.904 mM stock solution of **6** (25.4 mg, 0.0452 mmol, in dichloromethane) was prepared via volumetric pipet in a Schlenk tube. Then 10.00-mL aliquots of the stock solution were transferred by volumetric pipet into four Schlenk tubes containing different respective masses of $(PPN^+)Cl^-$: (a) 60.8 mg (0.106 mmol; $[(PPN^+)Cl^-]_o/[Ru{-}ONO_2]_o$ = 11.7), (b) 82.7 mg (0.144 mmol; $[(PPN^+)Cl^-]_o/[Ru{-}ONO_2]_o$ = 15.9), (c) 116.0 mg (0.2021 mmol; $[(PPN^+)Cl^-]_o/[Ru{-}ONO_2]_o$ = 22.4), (d) 125.7 mg (0.2190 mmol; $[(PPN^+)Cl^-]_o/[Ru{-}ONO_2]_o$ = 24.2). As soon as the reactants had dissolved, a portion of each mixture was transferred under N_2 by cannula into respective dry cuvettes; each cuvette was stoppered and placed into the thermostated cell-changer array set for 25.0 °C. After allowing 4 min for the solution to reach constant temperature, absorbance at 438 nm (decreasing) was recorded automatically every 24 s for 17.5 h. Since the reactions had not yet reached completion, the absorbance−time data were converted into ASCII format and imported into programs designed to estimate A_∞ values and then compute k_{obs} (FITEX for Mac[7a] and FINAL[7b] for PC). As a check on these values, the data were also imported into MS Excel and evaluated in standard pseudo-first-order fashion (linear regression of $\ln(A - A_\infty)$ versus time, discarding data past 3 half-lives when instrumental noise became significant) using the estimated A_∞ values. Values for k_{obs} were identical within 3% using the three methods. No pattern related to $[(PPN^+)Cl^-]_o$ was observed; values were scattered randomly (standard deviation 0.20×10^{-5}) around a mean of 4.37×10^{-5} s^{-1}.

IR Confirmation of Clean Conversion of Nitrate 6 into Chloride 1. A mixture of **6** (8.4 mg, 0.015 mmol) and $(PPN^+)Cl^-$ (25.3 mg, 0.045 mmol) in a Schlenk tube under N_2 was dissolved in 10.0 mL of dichloromethane. [A lower $[(PPN^+)Cl^-]_o/[Ru{-}ONO_2]_o$ ratio was used here to preclude interference from benzenoid overtone/combination bands of PPN^+.] A sample of the yellow-orange solution was transferred into a 5-mm CaF_2 cell, which was tightly sealed with Teflon stoppers. The solution was scanned automatically via macro control every 19 min. Spectral overlay (Figure 2) of selected scans showed clean isosbestic behavior. This technique was also used for the other nitrato complexes to confirm their clean conversion into their respective chloro analogues and the bromo analogue **11**.

Activation Parameters for Conversion of Nitrate 6 into Chloride 1. Multiple runs at 20.0 and 30.0 °C similar to those described above at 25.0 °C were carried out and analyzed to generate pseudo-first-order rate constants. Those experiments afforded values which also were apparently randomly scattered around their respective means of $2.82(11) \times 10^{-5}$ s^{-1} and $7.69(16) \times 10^{-5}$ s^{-1}. Values for $\Delta H^\ddagger$ and $\Delta S^\ddagger$ were determined from the regression analysis of an Eyring plot of $\ln(k/T)$ versus $1/T$ using the equations $\Delta H^\ddagger/R$ = − slope and $\Delta S^\ddagger/R$ = *y*-intercept.[8a] Uncertainties were calculated using MathCad.

Moisture Effect upon the Kinetics of Conversion of Nitrate 6 into Chloride 1. A reaction mixture of **6** (5.0 mg, 0.0090 mmol) and $(PPN^+)Cl^-$ (57.4 mg, 0.090 mmol) in 10.0 mL of dry dichloromethane was prepared using standard anhydrous techniques. A sample was transferred as usual into a dry cuvette, which was stoppered and inserted into the thermostated cell changer at 25.0 °C. The remainder of the solution was transferred via cannula under N_2 into an unheated 50-mL flask open to the atmosphere, a Teflon stirbar was added, the flask was fitted with rubber septum, and the solution was stirred 2 min. A 3-mL aliquot was transferred by unheated airtight syringe (Teflon plunger − exposure to relatively small glass surface area) into an unheated quartz cuvette, which was stoppered and inserted into the thermostated cell changer. The remaining solution was stirred another 5 min and then transferred, this time using a 10-mL all-glass syringe (exposure to large glass surface area) into another unheated quartz cuvette. It was also inserted into the cell changer, and absorbance at 438 nm was recorded automatically every 24 s for 17.5 h for all three samples. Pseudo-first-order rate constants were determined in a fashion identical to that described for anhydrous runs above, with values of $R^2 > 0.999$ found for all three.

Generation of (η^5-Cp)Ru(CO)(η^2-Ph_2P-C_6H_4-*o*-OMe)$^+$. To a solution of **4** (12.5 mg, 0.0240 mmol) in 15 mL of dichloromethane was added excess $AgBF_4$ (8.3 mg, 0.043 mmol). The mixture was stirred for 1.0 h in the dark and filtered through Celite. The resulting solution was somewhat darker than the initial solution of **4**. A 2-mL aliquot was taken for IR analysis. After the spectrum had been run, $(PPN^+)Cl^-$ (2.5 mg, 0.0047 mmol) was added to this aliquot, and the IR spectrum was recorded within 5 min of mixing. The remaining solution was concentrated to ca. 1 mL under reduced pressure.

(7) (a) Program from the Jack Norton group (then at Colorado State University) written by S. Kristjansdottir. (b) MathCad program by , A. Wierzbicki.

(8) Atwood, J. D. *Inorganic and Organometallic Reaction Mechanisms*, 2nd ed.; VCH: New York, 1997: (a) pp 13−14; (b) pp 153−155.

Attempts to isolate a solid by slowly adding 2 mLof diethyl ether followed by 10 mL of cyclohexane afforded an intractable tar.

Semiempirical Calculations. PM3(tm) calculations were conducted using the Spartan platform from Wavefunction, Inc. (either as PC−Spartan Pro, Spartan, or Jaguar).[9] The minimization routine was prohibited from using the pseudodiagonalization algorithm during the SCF procedure. The default fixed planar η^5-cyclopentadienyl group ligand from the menu was used unless otherwise specified. Where necessary, the $Ru-ONO_2$ distance was constrained to the value measured by X-ray crystallography for **6**. A variety of isomers of pseudooctahedral (η^3-Cp)Ru(CO)(η^2-Ph_2P(*o*-anisyl))ONO_2 were constructed by changing the relative locations of the P and O ligating atoms of η^2-Ph_2P(*o*-anisyl). From this effort, the lowest-energy isomer obtained upon PM3(tm) optimization was used for the analyses presented later.

Crystallography. Crystals of **1·toluene**, **2**, and **6** were sealed into thin-walled glass capillaries. Cell information and data collection were carried out on an Enraf Nonius CAD4 (**1** and **6**) and a Siemens R3m/v (**2**) diffractometer with monochromatized Mo Kα radiation (λ = 0.71073A). Intensity data were corrected for Lorentz and polarization effects. Structures were discovered with SHELXTL-PC[10] and SHELXS-97.[11] Information on the crystallographic experiments is given in Table 4

. Models included positions and anisotropic displacement factors for all non-H atoms and calculated H-atom positions and fixed isotropic displacement factors for H-atoms in appropriate geometries. Structures were refined by full-matrix least-squares methods against the intensities to convergence, with form factors taken from the standard source.[12] Data were also corrected for absorption effects using SHELXTL-PC and XEMP.[10] In **2**, a disorder in the locations of the Cl and carbonyl ligands was included in the model refinement with the major conformer having occupancy 0.893(8).

Results and Discussion

The complexes of formula (η^5-Cp)Ru(CO)(ER_3)ONO_2 were prepared in high yield by treating their chloro analogues with a slight excess of $AgNO_3$. The chloro

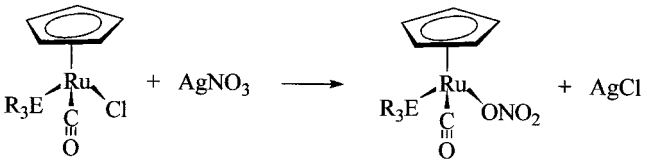

complexes were synthesized in high yield by heating (η^5-Cp)$Ru(CO)_2Cl$ with a slight excess of phosphorus or arsenic ligand in refluxing toluene.[6] Those containing PPh_3[5] and $P(OPh)_3$[6a] were reported earlier by other groups. IR and NMR data pertinent to structure and bonding considerations are reported in Table 1. As expected, $\nu_{C\equiv O}$ were higher (roughly 13 cm^{-1}) for the nitrato complexes than for their respective chloro analogues; such a pattern is typically observed for species with less electron density at the metal center available for donation into the CO π^* orbitals.[4,14] Similar patterns were seen for the ^1H and ^{13}C Cp resonances (about δ 0.05 and 0.6 higher, respectively for the nitrates than their chloride analogues).[15] $\nu_{C\equiv O}$, δ ^1H (Cp), and δ ^{31}P values for the PPh_2(*o*-anisyl) complexes **4** and **9** appear anomalously low given the donor strength of PPh_2(*o*-anisyl) relative to the other pnictogen ligands, perhaps consistent with the dramatically greater reactivity of **9**.

Table 1. Pertinent Spectroscopic Data for (η^5-Cp)Ru(CO)(ER_3)X

compd	ER_3	X	ν_{CO}[a]	δ ^{31}P[b]	δ ^1H (Cp)[c]	δ ^{13}C (Cp)[d]
1	$AsPh_3$	Cl	1958		4.93	83.2
6	$AsPh_3$	ONO_2	1971		4.98	82.5
2	PPh_3	Cl	1959	48.92	4.89	85.6 (2.9)
7	PPh_3	ONO_2	1972	50.21	4.94	85.0 (2.9)
3	P(*p*-anisyl)$_3$	Cl	1953	44.19	4.88	85.5
8	P(*p*-anisyl)$_3$	ONO_2	1967	45.50	4.93	84.9
4	PPh_2(*o*-anisyl)	Cl	1962	41.37	4.80	85.3
9	PPh_2(*o*-anisyl)	ONO_2	1974	43.75	4.87	84.5
11	PPh_2(*o*-anisyl)	Br	1961	41.15	4.79	85.5
5	$P(OPh)_3$	Cl	1988	−24.44	4.53	85.1 (2.9)
10	$P(OPh)_3$	ONO_2	1988	−22.33	4.66	84.5 (2.9)

[a] In CH_2Cl_2, cm^{-1}. [b] In $CDCl_3$, ppm above external 85% H_3PO_4. [c] In $CDCl_3$, ppm above TMS. [d] In $CDCl_3$, ppm above TMS; coupling constant to ^{31}P in parentheses.

Kinetics Studies of the Substitution of Chloride for Nitrate in Complexes 6−10. Under pseudo-first-order conditions (Cl^-/Ru ≥ 10), the nitrato complexes reacted smoothly with $(PPN^+)Cl^-$ to quantitatively afford their respective chloro analogues (eq 1).

$$(\eta^5\text{-Cp})Ru(CO)(ER_3)ONO_2 + (PPN^+)Cl^- \rightarrow (\eta^5\text{-Cp})Ru(CO)(ER_3)Cl + (PPN^+)ONO_2^- \quad (1)$$

Repetitive scans of reaction mixtures using UV−visible (550−350 nm) and IR spectroscopy (2020−1900 cm^{-1}) displayed clean isosbestic behavior. Respective examples are provided for reaction of complex **6** in Figures 1 and 2. Isosbestic points were observed at 465, 384, and 359 nm and at 1968 cm^{-1}, respectively. Similar results were obtained for reactions of the other nitrates, including those of **9** with $(PPN^+)Br^-$ to form the bromide **11**.

To determine the values of k_{obs} for each anion-metathesis reaction, the absorbance at ca. 440 nm of the anhydrous reaction mixture was recorded at short intervals at constant temperature. For example, the conversion of **6** to **1** was monitored at 438 nm, tracking the replacement of a more intense band for **6** (λ_{max} = 430 nm) with one less intense for **1** (λ_{max} = 448 nm). Only for the conversion of complex **9** was the reaction sufficiently fast to practically afford measured values of A_∞. For the others, absorbance−time data were imported into programs[7] using exponential fitting routines to generate estimates of A_∞ and then calculate values of k_{obs}. Combination of A_∞ values from these

(9) (a) PCSpartan Pro, version 1.01 and Spartan, version 5.1. Wavefunction, Inc., 18401 Von Karman Ave., Suite 370, Irvine, CA 92612. (b) Titan, version 1. Wavefunction, Inc., 18401 Von Karman Ave., Suite 370, Irvine, CA 92612; Schrodinger, Inc., 1500 SW First Avenue, Suite 1180, Portland, OR 97201.

(10) *Siemens SHELXTL-PC Manual*, V4.2; Siemens Analytical Instruments; Madison, WI, 1992.

(11) XEMP, 1989. Empirical Absorption Correction. Siemens Analytical X-ray Inc., 1989.

(12) Churchill, M. R. *Inorg. Chem.* **1973**, *12*, 1213.

(13) SHELXL-97/SHELXS-97. Sheldrick, G. Programs for solution and refinement of crystal structures from X-ray diffraction data, University of Göttingen, 1997.

(14) A similar pattern is observed for ν(N≡N) in *trans*-$Ir(PPh_3)_2(N_2)X$ complexes of the weakly coordinating trifluoracetate anion and chloride ion. Kubota, M.; Chappell, T. G.; Powers, S. P *Inorg. Chem.* **1979**, *18*, 3615.

(15) Kulawiec, R. J.; Faller, J. W.; Crabtree, R. H. *Organometallics* **1990**, *9*, 745 and references therein.

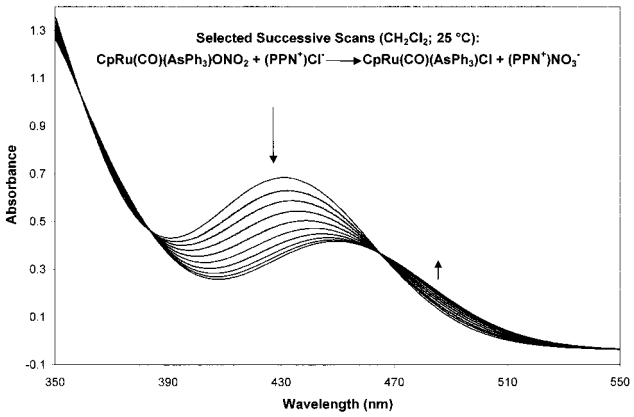

Figure 1. Selected successive UV−visible scans for conversion of nitrate **6** into chloride **1**.

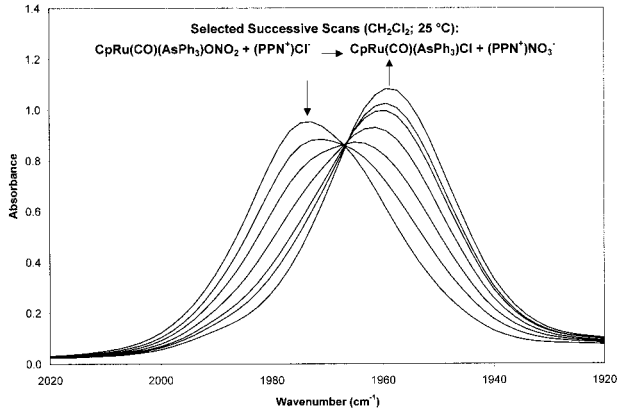

Figure 2. Selected successive FTIR scans for conversion of nitrate **6** into chloride **1**.

programs and the individual spectroscopic data in a standard spreadsheet pseudo-first-order linear-regression routine afforded similar numbers. Values for k_{obs} for a given run were always identical within 3% using the three methods. Each set of nitrate (**6**−**10**) into chloride metathesis experiments was run at 25 °C. That for **6** was also conducted at 20 and 30 °C to allow determination of activation parameters. Data appear in Table 2. Also included are results at 20 °C for the conversion of nitrate **9** into both its respective chloride **6** and bromide **11**. Those rates are identical within experimental error (i.e., no dependence upon either nature or concentration of entering halide, and $k_{obs} = k_1$). These results afford the rate expression rate = $k_1[(\eta^5\text{-Cp})Ru(CO)(ER_3)ONO_2]$.

First-order rate constants for nitrate metathesis in $CpRu(CO)(ER_3)ONO_2$ based upon ancillary pnictogen ligand ER_3 follow the order $P(OPh)_3 < PPh_3 < P(p\text{-anisyl})_3 < AsPh_3 \ll PPh_2(o\text{-anisyl})$. For the less reactive nitrate complexes containing phosphorus ligands, metathesis rate qualitatively follows ligand donor strength, with only a relatively small range exhibited. Such a trend can be rationalized in terms of a mechanism whose rate-determining step involves dissociation of nitrate from the coordination sphere to form a tight ion-pair. A stronger donor ligand can be pictured as (i) weakening the $Ru-ONO_2$ bond modestly by putting more electron density upon the Ru atom and (ii) somewhat better stabilizing the coordinatively unsaturated positively charged intermediate. The $AsPh_3$ complex seems somewhat anomalous, for it should be quite

Table 2. First-Order Rate Constants for Anhydrous Conversion of Nitrate to Halide Complex

complex	ligand	halide	temp (°C)	k (s^{-1})
6	$AsPh_3$	Cl^-	20.0	$2.82(11) \times 10^{-5}$
6	$AsPh_3$	Cl^-	25.0	$4.37(20) \times 10^{-5}$
6	$AsPh_3$	Cl^-	30.0	$7.69(16) \times 10^{-5}$
7	PPh_3	Cl^-	25.0	$2.10(18) \times 10^{-5}$
8	$P(p\text{-anisyl})_3$	Cl^-	25.0	$3.78(20) \times 10^{-5}$
9	$PPh_2(o\text{-anisyl})$	Cl^-	25.0	$4.90(10) \times 10^{-3}$
9	$PPh_2(o\text{-anisyl})$	Cl^-	20.0	$2.71(13) \times 10^{-3}$
9	$PPh_2(o\text{-anisyl})$	Br^-	20.0	$2.64(15) \times 10^{-3}$
10	$P(OPh)_3$	Cl^-	25.0	$1.40(21) \times 10^{-5}$

similar in reactivity to its PPh_3 analogue. Donor strength for $AsPh_3$ in binding to soft, low-valent metal moieties has been estimated in thermochemical studies[16] as just slightly less than that of PPh_3. $\nu_{C\equiv O}$ in $CpRu(CO)(EPh_3)X$ for both $X = ONO_2$ and Cl follow the trend $EPh_3 = P(OPh)_3 < PPh_3 < AsPh_3 < P(p\text{-anisyl})_3$. $P(p\text{-anisyl})_3$ appears to be a significantly stronger donor than $AsPh_3$ in this system, with $\nu_{C\equiv O}$ 4−5 cm^{-1} lower for complexes of the former (Table 1). Tertiary arsines are also slightly less sterically demanding than their phosphine analogues.[17] Thus, the presence of $AsPh_3$ in the coordination sphere should be less effective in a dissociative pathway than that of $P(p\text{-anisyl})_3$.

An Eyring plot of the data for conversion of the $AsPh_3$ complex **6** into **1** over the temperature range 20−30 °C afforded values of $\Delta H^{\ddagger} = 17(2)$ kcal/mol and $\Delta S^{\ddagger} = -21(5)$ eu, with $R^2 = 0.99$. [The slowness of the reaction and the volatility of solvent dichloromethane limited the temperature range available.] The moderately large negative entropy of activation argues strongly against a mechanism involving rate-determining dissociation of CO. It is, however, consistent with one in which nitrate leaves the coordination sphere to form an ion-pair in which nitrate is both tightly electrostatically attracted to the resulting CpRu cation and highly solvated by CH_2Cl_2 molecules. [Negative entropies of activation have been observed for anion metathesis using $(PPN^+)Cl^-$ in dichloromethane for $FeBr_4^{2-}$ and $CpMoI_2(PMe_3)_2$; however, unlike our situation, both reactions exhibit first-order dependence upon chloride concentration and would be expected to create transition states more ordered than the reactants alone.[18,19]]

The complex containing the *o*-OMe-substituted phosphine $PPh_2(o\text{-anisyl})$ was much more reactive than the rest of the set (k_1 over 2 orders of magnitudes greater). $\nu_{C\equiv O}$ appeared higher than expected for both its nitrato and chloro complexes based upon its substituents (Table 2), and its values for δ ^{1}H (Cp) and δ ^{31}P were similarly inconsistent. Unfortunately, multiple attempts to grow single crystals of **4** and **9** suitable for X-ray analysis failed. A likely explanation for the major difference in reactivity of **9** is stabilization of a coordinatively unsaturated intermediate by weak coordination of the potentially chelating *o*-OMe group. Shaw[20] publicized such chemistry extensively, and many similar types of bidentate hemilabile phosphorus ligands have been stud-

(16) Rottink, M. K.; Angelici, R. J. *Inorg. Chem.* **1993**, *32*, 3282 and references therein.
(17) Tolman, C. A. *Chem. Rev.* **1977**, *77*, 313
(18) Algra, G. P.; Balt, S. *Inorg. Chem.* **1981**, *20*, 1102.
(19) Poli, R.; Owens, B. E.; Linck, R. G. *Inorg. Chem.* **1992**, *31*, 662.
(20) Empsall, H. D.; Hyde, E. M.; Jones, C. E.; Shaw, B. L. *J. Chem. Soc., Dalton Trans.* **1974**, 1980.

Table 3. Selected Bond Lengths and Angles for Complexes 1·Toluene, 2, and 6

	complex		
	1·toluene	**2**	**6**
formula	$CpRu(CO)(AsPh_3)Cl$·toluene	$CpRu(CO)(PPh_3)C_l$	$CpRu(CO)(AsPh_3)ONO_2$
Ru-E (Å)	Ru(1)−As(1) = 2.412(1)	Ru(1)−P(1) = 2.3120(7)	Ru(1)−As(1) = 2.435(1)
Ru−C_{Cp} (Å)	Ru(1)−C(1) = 2.200(11)	Ru(1)−C(1) = 2.231(4)	Ru(1)−C(1) = 2.163(13)
	Ru(1)−C(2) = 2.221(12)	Ru(1)−C(2) = 2.15(3)	Ru(1)−C(2) = 2.185(12)
	Ru(1)−C(3) = 2.226(18)	Ru(1)−C(3) = 2.207(4)	Ru(1)−C(3) = 2.230(8)
	Ru(1)−C(4) = 2.169(14)	Ru(1)−C(4) = 2.185(4)	Ru(1)−C(4) = 2.243(7)
	Ru(1)−C(5) = 2.175(12)	Ru(1)−C(5) = 2.218(4)	Ru(1)−C(5) = 2.222(8)
Ru−C_{co} (Å)	Ru(1)−C(0) = 1.862	Ru(1)−C(0) = 1.872(6)	Ru(1)−C(0) = 1.852(8)
E−C (Å)	As(1)−C(11) = 1.935(9)	P(1)−C(11) = 1.824(2)	As(1)−C(11) = 1.939(6)
	As(1)−C(21) = 1.931(8)	P(1)−C(21) = 1.822(2)	As(1)−C(21) = 1.934(5)
	As(1)−C(31) = 1.931(8)	P(1)−C(31) = 1.824(3)	As(1)−C(31) = 1.951(8)
C≡O (Å)	C(0)−O(0) = 1.15	C(0)−O(0) = 1.132(8)	C(0)−O(0) = 1.139(10)
C−C (Å)	C(1)−C(2) = 1.363(23)	C(1)−C(2) = 1.410(8)	C(1)−C(2) = 1.426(15)
	C(1)−C(5) = 1.344(17)	C(1)−C(5) = 1.374(8)	C(1)−C(5) = 1.386(20)
	C(2)−C(3) = 1.408(22)	C(2)−C(3) = 1.349(8)	C(2)−C(3) = 1.472(20)
	C(3)−C(4) = 1.380(22)	C(3)−C(4) = 1.363(8)	C(3)−C(4) = 1.351(15)
	C(4)−C(5) = 1.403(25)	C(4)−C(5) = 1.397(8)	C(4)−C(5) = 1.373(15)
other bond distances (Å)	Ru(1)−Cl(1) = 2.455(2)	Ru(1)−Cl(1) = 2.332(18)	Ru(1)−O(1) = 2.113(6)
			N(1)−O(1) = 1.294(7)
			N(1)−O(2) = 1.209(12)
			N(1)−O(3) = 1.212(11)
angles about Ru (deg)	As(1)−Ru(1)−Cl(1) = 90.7(1)	P(1)−Ru(1)−Cl(1) = 90.45(3)	As(1)−Ru(1)−O(1) = 86.9(1)
	As(1)−Ru(1)−C(0) = 88.7(3)	P(1)−Ru(1)−C(0) = 88.19(12)	As(1)−Ru(1)−C(0) = 90.0(2)
	Cl(1)−Ru(1)−C(0) = 93.0(3)	Cl(1)−Ru(1)−C(0) = 92.78(15)	O(1)−Ru(1)−C(0) = 97.8(3)
angle in carbonyl ligand (deg)	Ru(1)−C(0)−O(0) = 176.3(8)	Ru(1)−C(0)−O(0) = 178.3(8)	Ru(1)−C(0)−O(0) = 173.8(9)

ied, including the Shell Higher Olefin Process industrial application.[21] Kulawiec et al.[14] have reported complexes of formula (η^5-Cp)Ru(CO)(η^2-PPh_2(*o*-XC_6H_4))$^+$, where X = Cl or Br but not F, analogous to our postulated intermediate (η^5-Cp)Ru(CO)(η^2-PPh_2(*o*-$MeOC_6H_4$))$^+$. Evidence for our intermediate species was obtained by stirring chloro complex **4** with an excess of $AgBF_4$ in CH_2Cl_2. A white precipitate formed, and the $\nu_{C\equiv O}$ band shifted from 1962 to 1985 cm^{-1}. Such a frequency shift (+23 cm^{-1}) is appropriate for the OMe-coordinated cation, given that the *o*-OMe ligand should be a significantly better donor than the *o*-Br and *o*-Cl ligands. [Larger frequency shifts, 1971 to 2014 cm^{-1}, were observed by Kulawiec et al. upon stirring (η^5-Cp)-Ru(CO)(η^1-PPh_2(2-XC_6H_4))Cl with excess $AgPF_6$.]

The effect of small amounts of water upon the reaction rate was demonstrated by running the kinetics experiments with some exposure to atmospherically derived moisture. Allowing progressively more contact of the reaction mixture with unheated glass surfaces as described in the Experimental Section caused no change in rate law but did increase the value of k_{obs} (in multiples of 10^{-5} s^{-1}) from 4.33 to 5.11 to 5.51 at 25 °C. The value of k_{obs} never increased beyond 5.8×10^{-5} s^{-1}, no matter how wet the solvent was allowed to become. Similar results were observed in enhancement of metathesis for all the nitrates. This effect can be rationalized easily in terms of the proposed rate-determining step as conversion of coordinated nitrate to ion-paired nitrate. Water would likely hydrogen-bond to coordinated nitrate, weakening the Ru−ONO_2 bond and stabilizing the ion-pair intermediate in the weakly polar solvent dichloromethane.[22]

Crystal Structure of Complex 6. The crystal structure consists of an ordered arrangement of discrete molecular units, which are separated by normal van der Waals distances. There are no abnormally short intermolecular contacts. Molecular geometry of this complex is depicted in Figure 3; selected distances and angles are presented in Table 3 and crystallographic data in Table 4. The geometry around the ruthenium(II) is best described as a "three-legged piano-stool" conformation. The individual Ru−C(η^5-C_5H_5) distances ranged from Ru(1)−C(1) = 2.163(13) Å to Ru(1)−C(4) = 2.243(7) Å. The C−C distances associated with the cyclopentadienyl ring ranged from 1.351(15) to 1.472(20) Å. The three "legs" of this molecule were composed of a terminal carbonyl, a nitrate, and a triphenylarsine ligand, with the angles about these substituents relatively close to 90°. The environment around the arsenic atom was a somewhat distorted tetrahedron, with ∠Ru−As−C 116(1)° and ∠C−As−C 102(1)°, with distortion likely due to the bulkiness of the Ru moiety. Complete crystallographic data are available in the Supporting Information.

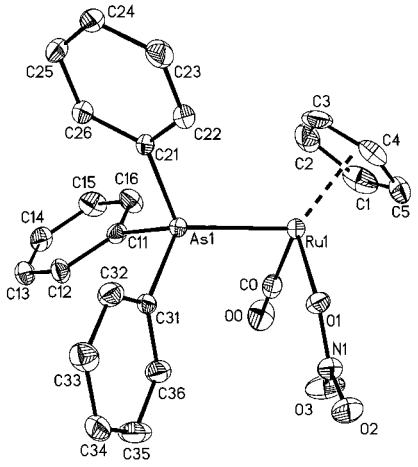

Figure 3. Thermal ellipsoid plot of complex **6** with 50% probablility enclosures.

(21) Parshall, G. W.; Ittel, S. D. *Homogeneous Catalysis*, 2nd. ed.; Wiley: New York, 1992; pp 70−71.

(22) We earlier observed strong perturbation of an equilibrium involving Rh−F. Branan, D. M.; Hoffman, N. W.; McElroy, E. A.; Miller, N. C.; Ramage, D. L.; Schott, A. F.; Young, S. H. *Inorg. Chem*. **1987**, *26*, 2915.

Table 4. Crystallographic Details for 1·Toluene, 2, and 6

	complex		
	1·toluene	**2**	**6**
formula	$C_{31}H_{28}AsOClRu$	$C_{24}H_{20}POClRu$	$C_{24}H_{20}AsNO_4Ru$
fw	628.0	491.9	562.4
size (mm)	0.4, 0.25, 0.25	0.5, 0.2, 0.15	0.3, 0.25, 0.25
system	monoclinic	triclinic	triclinic
space group	*P*2(1)/*c* (No. 14)	*P*-1 (No. 2)	*P*-1 (No. 2)
a	17.228(4)	9.381(2)	10.253(3)
b	7.831(1)	10.589(2)	10.760(1)
c	19.718(2)	11.534(2)	11.959(3)
α	90	76.64(2)	69.25(1)
β	110.84(2)	79.20(2)	68.00(2)
γ	90	78.33(2)	69.51(2)
V	2486(1)	1079.7(4)	1107.4(6)
Z (molecules/cell)	4	2	2
density	1.678	1.513	1.687
trans. coeff. (max, min)	0.83, 0.67	0.87, 0.65	0.64, 0.25
F(000)	1264	496	560
θ range, *hkl* range	2.5−22.5 18; 7; ±21	1.8−32.5 14;±16;±17	2.5−22.5 11;±11;±12
scan type	*ω*	*ω*	*ω*−2*θ*
intensities measd	3299	9241	3071
unique refl. (R_{merge})	3179 (3.9%)	7824 (4.0%)	2880 (4.5%)
obsd reflns (cutoff)	2302 ($I > 2\sigma I$)	5655 ($I > 2\sigma I$)	2519 ($I > 2\sigma I$)
parameters	269	267	281
R, wR (observed)	0.0470, 0.0572	0.0446, 0.0973	0.0600, 0.0599
R, wR (all data)	0.0716, 0.0779	0.0708, 0.1085	0.0654, 0.0698
goodness-of-fit	0.95	1.03	0.82
data/parameter ratio	8.6	29.3	10.2
diff map features	+0.96, −1.40	+0.86, −0.87	+2.09, −1.49

Crystal Structure of Complex 1. A toluene molecule of solvation was present in the crystal structure. This solvent molecule exhibited static disorder. The disorder pattern can be easily rationalized as the averaging of two distinct toluene molecules which are related by a 180° rotation. The resultant averaged electron density possessed a center of symmetry. The six-membered toluene ring was treated as fixed hexagon during refinement. There was also static disorder associated with the arrangement of the $CpRu(CO)(AsPh_3)$-Cl molecules in the crystal structure. Minor scrambling between the carbonyl and chloro ligands of each molecule was observed. Unfortunately, this disorder manifested itself as an impossibly short C−O bond length of 1.012(16) Å. All attempts to model the disorder were unsuccessful due to the resolution of the study. The final structure is reported with the distances associated with the carbonyl fixed at "reasonable" distances. The C0−O0 and Ru1−C0 bond distances were constrained respectively to interatomic distances of 1.15 and 1.862 Å. The resulting structure modeled the actual electron density and the refinement converged (largest Δ/σ = 0.023, which was related to the disordered toluene solvent molecule) with $R = 0.0470$ and $wR = 0.0572$ for those 2302 reflections with $F_o > 4\sigma(F_o)$. The final difference Fourier map showed no anomalous features after refinement, with the residual electron density in the range −1.40 to 0.96 e $Å^{-3}$. The ORTEP diagram appears as Figure 4, and pertinent structural data are presented in Tables 3 and 4. Complete crystallographic data are available in the Supporting Information.

Crystal Structure of Complex 2. We decided to obtain a new crystal structure of **2** because the original[23] displayed an *R* factor above 0.10 and we wished to compare the PM3(tm)-computed structure with an experimentally determined structure of higher quality.

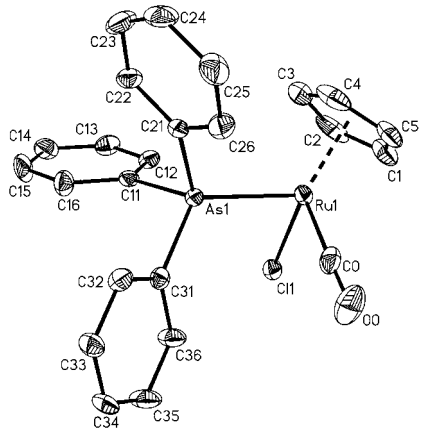

Figure 4. Thermal ellipsoid plot of complex **1**·toluene with 50% probablility enclosures.

In the later stages of model refinement, it became clear that the carbonyl and chlorine groups were disordered. [The carbonyl bond length was very short; in fact, much shorter than the 1.145(20) Å typical of most carbonyl complexes.] Although the Fourier difference map showed residual peaks in the vicinity of the metal atom and the carbonyl group, an empirical absorption correction failed to eliminate the features near the carbonyl. Since the Ru−Cl and Ru−(CO) distances were similar, a model in which a disorder in the Cl and CO groups occurred was examined, with immediate improvement in the model. The model with contributions from this disorder converged with a major conformer having a site occupancy of 0.893(8). The C−O bond length (of the major isomer) became 1.132 Å. The alternate Cl, C, and O atoms were modeled with isotropic displacement factors, and the metrics associated with them were close to their isomeric counterparts with an appropriate increase in errors since their density was small. Final R [$I > 2\sigma(I)$] = 0.0446, $wR_2 = 0.0973$, and for all data $R_1 = 0.0708$, $wR_2 = 0.1085$. The ORTEP diagram appears as Figure

(23) Wilczewski, T.; Dauter, Z. *J. Organomet. Chem.* **1986**, *312*, 349.

Table 5. Comparison of (η^5-Cp)Ru(CO)(ER_3)X Crystal and Computed Structures

ER_3	X	Ru−CO	CO	Ru−ER_3	Ru−X	∠X−Ru−E	∠X−Ru−C	∠C−Ru−E
$AsPh_3$ (crystal)	NO_3	1.852(8)	1.139(10)	2.485(1)	2.113(6)	86.9(1)	97.8(3)	90.0(2)
$AsPh_3$ (PM3(tm)[b])	NO_3	1.872	1.177	2.459	2.113/fixed	89.0	96.5	91.1
$AsPh_3$·toluene (crystal)[c]	Cl	1.862[c]	1.15[c]	2.412(1)	2.455(2)	90.8(1)	92.6(3)	88.5(3)
$AsPh_3$ (PM3(tm))	Cl	1.856	1.182	2.448	2.323	89.94	89.31	91.78
PPh_3 (crystal)[d]	Cl	1.872	1.132	2.312	2.401	90.45	92.77	88.18
PPh_3 (PM3(tm))	Cl	1.856	1.182	2.253	2.331	91.9	90.24	92.57

[a] Experimental and calculated bond lengths and angles are reported in angstroms and degrees, respectively. [b] Ru−ONO_2 bond constrained at 2.11 Å. [c] Carbonyl/chloro disorder afforded unrealistically short CO bond length of 1.012(16) Å, so Ru−C and CO arbitrarily were assigned more reasonable values on the basis of Cambridge Structural Databased carbonyl/chloro disorder observed here, but structure solution parameters allowed theoretically reasonable values for Ru−C and CO bond lengths.

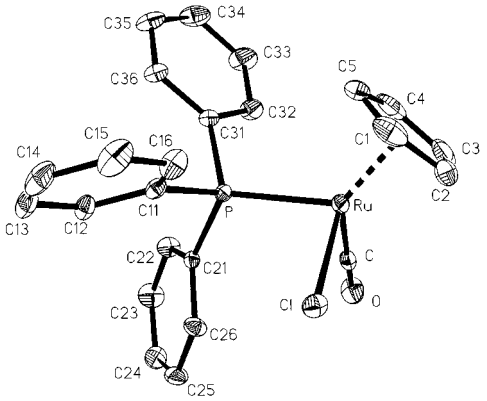

Figure 5. Thermal ellipsoid plot of complex **2** with 50% probablility enclosures.

5, and pertinent structural data are presented in Tables 3 and 4. Complete crystallographic data are available in the Supporting Information.

Semiempirical PM3(tm) Computational Studies. A comparison of X-ray and PM3(tm) semiempirical structural data (Table 5) for the complexes available (**1**, **2**, and **6**) showed reasonable agreement between the two. The computed structures display Ru−CO slightly short, C≡O somewhat too long, Ru−Cl moderately too short, and bond angles quite acceptable. For **6** it was necessary to constrain the Ru−O bond to keep the nitrate group from dissociating to noncovalent distances (ca. 4.6 Å). The *Ru*−ONO_2 distance was set to 2.113 Å, the value observed in its crystal structure. With the same minimization routine in place, the other nitrato species did not dissociate the nitrate group but placed it considerably farther away than seen in the $AsPh_3$ complex crystal structure (from 2.33 Å for **8** to 2.18 Å for **10**). To get a better prediction of structures, we also constrained the Ru−O bond distances in **7**−**10** to essentially that in the crystal structure of **6**.

Within the set of computed structures, very small differences in Ru−C and Ru−Cl bond distances were observed for chlorides **1**−**4**, and Ru−P distances were very similar for **2**−**4**. The computed $P(OPh)_3$ chloride **5**, however, displayed Ru−C 0.02 Å longer and Ru−P 0.03 Å shorter than did its phosphine analogues. The set of computed nitrates showed modest differences in two bond distances relative to the computed chlorides: Ru−C ca. 0.01 Å longer and Ru−E slightly longer (0.005−0.01 Å longer). Computed bond angles around Ru were similar for the two sets. Pertinent data are summarized in the Supporting Information.

If one assumes that the ion-pairing electrostatic interactions between (η^5-Cp)Ru(CO)(ER_3)$^+$ and nitrate ion are very similar in strength for all ER_3, relative $\Delta H^{\ddagger}$ for our proposed mechanism for the nitrate-to-chloride metatheses can be estimated by comparing the differences in computed energies (standard heats of formation) for the nitrato complexes and the (η^5-Cp)Ru(CO)(ER_3)$^+$ intermediates. Although the absolute energies for complexes are not accurate, differences between energies in pairs of species structurally related like those here are considered to be qualitatively meaningful.[24] Pertinent data appear in Table 6. Two entries appear for the Ph_2P(*o*-anisyl) nitrate **9** to show the effect of chelation by the *o*-OMe group. The values in general are quite similar, but two points stand out: (i) the considerably higher value for the $P(OPh)_3$ system (the least reactive nitrate) and (ii) the significantly lower value for the chelated Ph_2P(*o*-anisyl) system.

Table 6. Computed Heats of Formation of Nitrate Complexes and Proposed Cation Intermediates

ER_3	ΔH_f of nitrate complex (kcal/mol)	ΔH_f of proposed cation intermediate (kcal/mol)	difference (kcal/mol)
$AsPh_3$	−94.272	41.844	136.116
PPh_3	−145.782	−9.588	136.194
$P(p\text{-anisyl})_3$	−260.656	−127.211	133.445
PPh_2(*o*-anisyl)	−175.056	(η^1-PPh_2(*o*-anisyl)) −42.929	132.127
PPh_2(*o*-anisyl)	−175.056	(η^2-PPh_2(*o*-anisyl)) −47.627	127.429
$P(OPh)_3$	−318.573	−171.731	146.842

[a] Calculated heats of formation determined using PM3(tm)-optimized geometries.

To address the considerably greater reactivity of the Ph_2P(*o*-anisyl) nitrate **9** in more detail, we computed a series of structures. (η^5-Cp)Ru(CO)(η^1-L)ONO_2 with unconstrained *Ru*−ONO_2 distance afforded an unexpected species in which the nitrate anion is apparently dissociated without significant bonding of the *o*-OMe group to Ru: *Ru*−ONO_2 = 4.73 Å and *Ru*−*O*Me = 4.149 Å. Constraining *Ru*−ONO_2 to 3.50 Å, a distance observed without constraint for the PPh_3 analogue, raised the energy by 10 kcal/mol for the geometry-optimized structure but reduced *Ru*−*O*Me only to 4.13 Å. Removing the nitrate anion completely without mechanically forming a Ru−OMe bond afforded a coordinatively unsaturated cation with *Ru*−*O*Me distance of 3.233 Å and an energy of −42.93 kcal/mol. Mechanically forming a Ru−OMe bond yielded an η^2 coordina-

(24) (a) Adam, K. R.; Atkinson, I. M.; Lindoy, L. F. *J. Mol. Struct.* **1996**, *384*, 183. (b) Børve, K. J.; Jensen, V. R.; Karlsen, T.; Støvneng, J. A.; Swang, O. *J. Mol. Model.* **1997**, *3*, 193. (c) Decker, S. A.; Donini, O.; Klobukowski, M. *J. Phys. Chem. A* **1997**, *101*, 8734. (d) Cundari, T. R.; Saunders:, L. C.; Sisterhen, L. L. *J. Phys. Chem.* **1998**, *102*, 997. (e) Donovan-Merkert, B. T.; Clontz, C. R.; Rhinehart, L. M.; Tijong, H. I.; Carlin, C. M.; Cundari, T. R.; Rheingold, A. L.; Guzei, I. *Organometallics* **1998**, *17*, 1716. (f) Decker, S. A.; Klobukowski, M. *Can. J. Chem.* **1999**, *77*, 65. (g) Cundari, T. R.; Deng, J. *J. Chem. Info. Comput. Sci.* **1999**, *39*, 376. (h) Cundari, T. R.; Deng, J. *Intern. J. Quantum Chem.* **2000**, *77*, 421.

Table 7. Computed Effects for η^1 to η^2 Conversion of $(\eta^5\text{-Cp})Ru(CO)(Ph_2P(o\text{-}XC_6H_4))^+$

						$\eta^1 \rightarrow \eta^2$ changes		
X[a]	r(Ru−X) (Å)	r(Ar−X) (Å)	ΔH_f (kcal/mol)	∠Ru−X−Ar (deg)	X	Δ(Ru-X) (Å)	Δ(Ar-X) (Å)	Δ(ΔH_f) (kcal/mol)
η^1−Br	3.169	1.894	3.245	NA				
η^1−Cl	4.463	1.698	−6.298	NA				
η^1−F	4.179	1.347	−43.415	NA	Br	−0.515	0.014	−5.824
η^1−OMe	5.385	1.376	−42.929	NA	Cl	−2.519	0.025	−23.395
η^2−Br	2.654	1.908	−2.579	94.3	F	−0.591	0.000	0.140
η^2−Cl	2.304	1.723	−29.693	108.4	OMe	−1.833	0.027	−4.698
η^2−F	3.588	1.347	−43.275	94.0				
η^2−OMe	3.552	1.406	−47.627	97.5				

[a] Calculated metrics and heats of formation determined using the PM3(tm) semiempirical Hamiltonian.

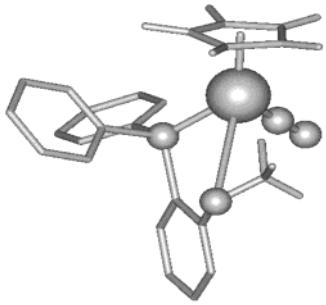

Figure 6. Computed η^2 coordinatively saturated cation with a very weak Ru−OMe bond.

tively saturated cation (Figure 6) with a very weak Ru−OMe bond (3.55 Å) about 5 kcal/mol lower in energy than the former. The η^2-isomer is essentially isoelectronic to the halo-substituted aryl species $(\eta^5\text{-Cp})Ru(CO)(\eta^2\text{-}Ph_2P(o\text{-}XC_6H_4))^+$ characterized by Kulawiec et al.[15] Computations of structures for the η^1 and η^2 isomers for X = Br, Cl, and F showed no stabilization upon η^1 to η^2 conversion for X = F (matching their experimental observations), considerable stabilization for X = Cl, and stabilization for X = Br comparable to that for X = OMe. Considerably shorter Ru−X bonds were computed for X = Cl and Br (reasonably close to values such as those reported in crystallographic data for η^2-bound haloarene ligands[15]) than for X = OMe. Pertinent parameters are presented in Table 7.

A path by which complex **9** might dissociate the nitrate anion was suggested from computed structures for the two isomers (Figure 7) of coordinatively saturated $(\eta^3\text{-Cp})Ru(CO)(\eta^2\text{-}Ph_2P(o\text{-}MeOC_6H_4))ONO_2$, which could be generated from **9** by Cp ring slippage.[8b] [Both isomers displayed no imaginary frequencies when vibrations were calculated, a fact showing that neither corresponds to a transition state.] The P-equatorial form, 19 kcal/mol more stable than its P-axial isomer, had elongated *Ru*−*O*NO_2 (3.50 Å) and *Ru*−*O*Me (3.40 Å). Return of the Cp ring from η^3- to η^5-form could expel nitrate from the coordination sphere to generate the putative ion-paired intermediate $(\eta^5\text{-Cp})Ru(CO)(\eta^2\text{-}Ph_2P\text{-}(o\text{-}MeOC_6H_4))^+$.

Conclusion

The kinetics studies on the chloride-for-nitrate metathesis carried out for this set of five d^6 $(\eta^5\text{-Cp})Ru(CO)(ER_3)ONO_2$ showed that the stereoelectronic nature of the ancillary pnictogen ligand has a relatively minor effect upon reactivity. Four factors argue strongly for a mechanism in which nitrate ion dissociates from the ruthenium coordination sphere to generate a coordina-

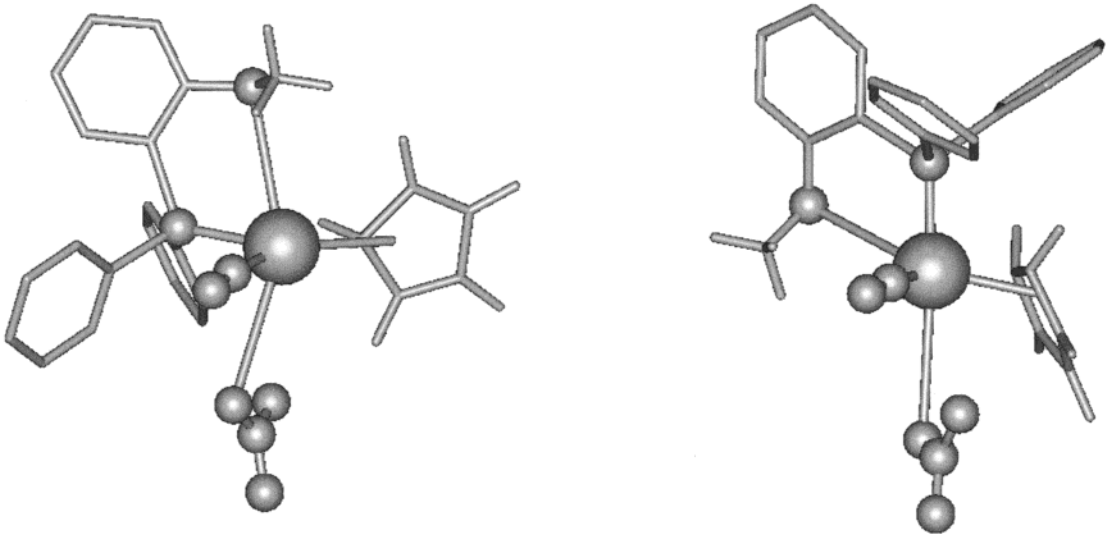

P-equatorial $(\eta^3\text{-Cp})Ru(CO)(\eta^2\text{-}Ph_2P(o\text{-}MeOC_6H_4))ONO_2$ **P-axial $(\eta^3\text{-Cp})Ru(CO)(\eta^2\text{-}Ph_2P(o\text{-}MeOC_6H_4))ONO_2$**

(phenyl hydrogens omitted for clarity)

Figure 7. Computed isomers of coordinatively saturated $(\eta^3\text{-Cp})Ru(CO)(\eta^2\text{-}Ph_2P(o\text{-}MeOC_6H_4))ONO_2$ generated via Cp ring slippage.

tively unsaturated highly solvated contact ion-pair: (a) the form of rate law observed (first-order in [CpRu−ONO_2], zero-order in chloride and bromide), (b) the rate enhancement without change in form of rate law caused by traces of water, (c) the moderately large negative entropy of activation, (d) and the very large rate enhancement stemming from the presence of the *o*-methoxy group in the Ph_2P(*o*-anisyl) ligand. Semi-empirical PM3(tm) calculations modeled the reactants and products reasonably well on the basis of comparisons of geometry-optimized structures with X-ray crystal structures, and computed putative intermediates were logical in terms of energetics and structural parameters.

Acknowledgment. N.W.H. acknowledges support from Research Corporation and the Petroleum Research Fund, administered by the American Chemical Society, and thanks Dr. Alan Salter for helpful discussions. T.R.C. wishes to acknowledge the National Science Foundation for their support of equipment (CHE-9785017) and facilities (STI-9602656) improvements for the CROMIUM research laboratories. E.A.V. thanks the Office of Naval Research for instrumentation support.

Supporting Information Available: Complete structure reports including atomic coordinates, thermal parameters, and bond lengths and angles for the crystal structures of **1**, **2**, and **6** and the Eyring plot for conversion of nitrate **6** into chloride **1**. This material is available free of charge via the Internet at http://pubs.acs.org. Complete atomic coordinates, thermal parameters, and bond lengths have been deposited at the Cambridge Crystallographic Data Centre. CCDC refs: 157617, 157697, and 157618. This information is also available free of charge via the Internet at http://pubs.acs.org.

OM000670D